Fused Bis-Azacalixphyrin that reaches NIR II absorptions

Lucien Lavaud, Cloe Azarias, Gabriel Canard, Simon Pascal, Joachim Galiana, Michel Giorgi, Zhongrui Chen, Denis Jacquemin, Olivier Siri

Fused Bis-Azacalixphyrin that reaches NIR II absorptions

Lucien Lavaud,[a] Cloé Azarias,[b,c] Gabriel Canard,*[a] Simon Pascal,[a] Joachim Galiana,[a] Michel Giorgi,[d] Zhongrui Chen,[a] Denis Jacquemin*[b] and Olivier Siri*[a]

[a.] *Aix Marseille Univ, CNRS, CINAM, UMR 7325, Centre Interdisciplinaire de Nanoscience de Marseille, Campus de Luminy, 13288 Marseille cedex 09, France. E-mails : gabriel.canard@univ-amu.fr; olivier.siri@univ-amu.fr*
[b.] *Laboratoire CEISAM, CNRS UMR 6230, Université de Nantes, 2, rue de la Houssinière, 44322 Nantes, France. E-mail : Denis.Jacquemin@univ-nantes.fr*
[c.] *Present address : LaboLife France, 1, rue François Bruneau, 44000 Nantes, France.*
[d.] *Aix Marseille Univ, CNRS, Centrale Marseille, FSCM, Spectropole, Marseille, France.*
† Electronic Supplementary Information (ESI) available: experimental protocols, ^{1}H and ^{13}C NMR spectra, theoretical details and further DFT/TD-DFT analyses.

The fusion of two azacalixphyrin cycles absorbing in the NIR-I domain moves the absorption properties beyond 1000 nm, towards the second biological transparency window (NIR-II). The synthesis of this new type of NIR-II dyes was achieved through the intermediate preparation of a rare example of bis-tetra-azacalix[4]arene where the two macrocycles share a common aromatic unit.

The design of organic dyes absorbing and/or emitting light in the near-infrared domain (NIR, 780-2000 nm) is continuously attracting great attention because such chromophores have numerous applications in, e.g., organic electronics[1] including the NIR to visible upconversion,[2] photocatalytic production of hydrogen,[3] preparation of panchromatic dye-sensitized solar cells[4] or photodetectors,[5] OLED emitting in the NIR,[6] and optical power limiting at telecommunications wavelengths.[7] The intense research of efficient NIR dyes has also been motivated by biological applications since the NIR region includes transparency windows of biological media found between 700 and 900 nm for the first (NIR-I) and between 1000 and 1700 nm for the second (NIR-II). These windows promoted the use of NIR dyes for optical imaging,[8] photodynamic therapy,[9] as well as the emerging non-invasive photoacoustic imaging (PAI).[9,10] For the later, non-fluorescent far-red and NIR dyes displaying a high molar absorptivity are particularly sought as PAI contrast agents. Among the numerous dyes absorbing in the far-red domain,[11] phthalocyanine or porphyrinoïd derivatives have been extensively studied because judicious modifications of their skeleton and/or of their aromatic conjugation pattern often induce large redshifts of their absorption bands.[4,11] In this context, we described in 2013 the synthesis of the first example of a pyrrole-free porphyrin analogue, azacalixphyrin 1[13] (ACP, Fig. 1) which can be described as a tetraaza-tetrabenziporphyrin[14] displaying an 18 π electron aromatic system and developing a bis-zwitterionic character. This compound, only soluble in highly polar solvents (MeOH, DMSO), features a panchromatic light-absorption from the UV to the NIR-I domain with a maximum of 886 nm (in a TFA-MeOH solution).[‡] The potential and features of the ACP architecture have been deeply investigated *in silico*,[15] and recently, the synthesis of ACPs presenting peripheral N-substituents allowed to sensibly increase their solubility and to further redshift their absorptions with maxima located at 894 nm for the tetra-N-octyl derivative 2[16] and up to 941 nm for the tetra-N-aryl ACP 3.[17] This latter compound showed promising results as a PAI contrast agent using a NIR excitation. Inspired by the fusion of porphyrins that allows fascinating absorption in the NIR domain (fused bis-porphyrins absorb typically at ca 1060 nm with ε ~ 23 000 $M^{-1}cm^{-1}$),[18] we describe here the synthesis and characterization of the first fused azacalixphyrin dimer 4 (bis-ACP) showing an intense absorption band beyond 1000 nm (Fig. 1).
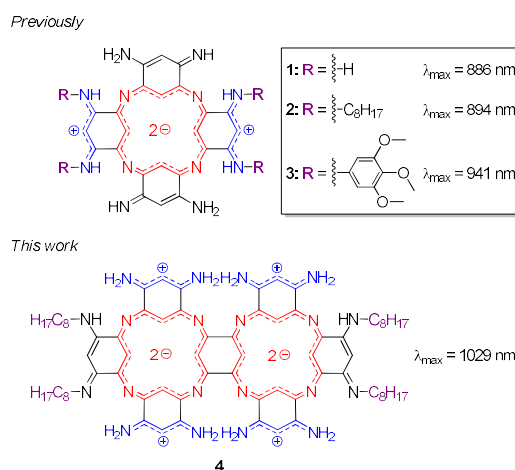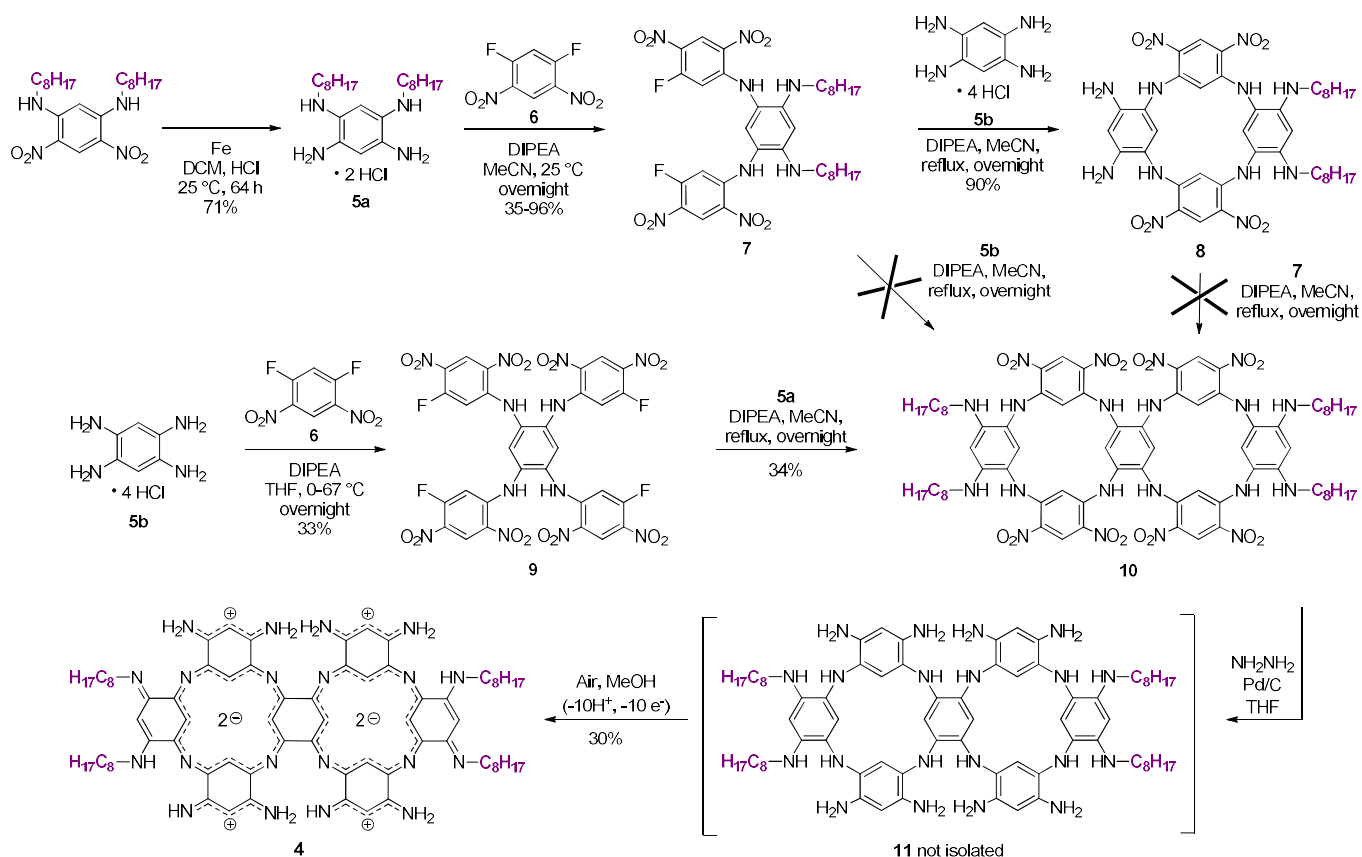

Fig. 1. Chemical structures of the neutral forms of ACPs **1-3** and of the fused bis-ACP **4** (with the corresponding maxima in the NIR domain recorded in TFA-MeOH solutions).[‡]

Scheme 1. Synthetic routes to the fused-ACP **4**.

Three strategies were explored to prepare the fused azacalixphyrin dimer **4** (Scheme 1). The synthesis of the key intermediate bis-azacalixarene **10** was envisaged either from the reactive tetraaminobenzene derivatives **5a** or **5b** that feature a good air-stability when stored as di-hydrochloride salts (Scheme 1). Using a synthetic pathway similar to the one allowing the preparation of N-substituted azacalixphyrins (**2** and **3**),[17] the adduct **7** was produced by the Nuleophilic Aromatic Substitution (SNAr) of the *N,N*-dioctyl tetraaminobenzene hydrochloride **5a** on two equivalents of 1,3-difluroro-4,6-dinitrobenzne **6** in the presence of *N,N*-diisopropylethylamine (DIPEA). Despite investigating multiple experimental conditions, the subsequent SNAr between two equivalents of **7** and one equivalent of the unsubstituted tetraaminobenzene **5b** afforded only the bis-*N*-octyl-azacalixarene **8**, that is produced with a high yield of 90% from an equimolar mixture of the starting derivatives.[16] This result was a first proof of the poor nucleophilic character of the remaining primary amine groups of **8** that does not react as well with **7** irrespective of the applied experimental conditions (variation of the solvent, the base, the temperature, or using microwaves). This weak nucleophilicity was confirmed by DFT calculations to be an electronic and not a geometric effect (see the ESI†), which indicated that another synthetic route had to be selected.

To circumvent the dead-end formation of the "inert" macrocycle **8**, a third and successful strategy was followed (Scheme 1). The SNAr involving **6** and **5b** in a 4 to 1 ratio produces the [1+4] adduct **9** whose single crystal X-ray structure has been solved (see the ESI†). The yield of this synthetic step is quite high (33%) regarding the successive SNAr that decrease the nucleophile strength of the remaining primary amine groups. The subsequent and stoichiometric condensation of **5a** on **9** leads to the expected bis-tetraazacalix[4]arene **10** with a yield of 34%.

The bismacrocycle **10** is one of the rare examples of a bis-calixarene derivative where the two macrocycles share an aromatic building block.[19] This key intermediate could be fully characterized including by X-ray analysis. As observed for azacalix[4]arene monomers,[20] each of the two macrocycles in **10** adopt an 1,3-alternate conformation originating from two elements. The first is the presence of eight intramolecular hydrogen bonds between the nitro groups and the acidic hydrogen atom borne by each of the bridging nitrogen atoms (Fig. 2.). The second origin is the sp^2 hybridization of the bridging N-atoms that are effectively conjugated with their adjacent di-nitroaryl moieties (short N-C average bond lengths of 1.36 Å). As can be seen in the left panel of Fig. 2, the molecule globally adopts a S-shape. A detailed DFT conformational investigation of **10** can be found in the ESI†, and indicates that several conformers globally similar to the one obtained by X-Ray are likely coexisting in solution.
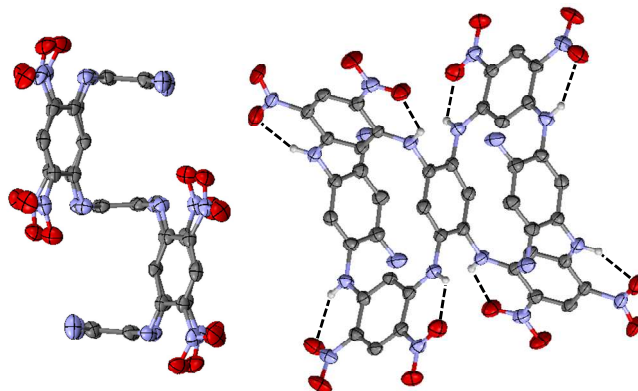
2

Fig. 2. Two views of the single-crystal X-ray structure of **10** showing the bis-1,3-alternate conformation and the intramolecular $NO_2\cdots HN$ hydrogen bonds (aromatic hydrogen atoms and octyl chains are omitted for clarity).

The reduction of the eight nitro groups of **10** was conducted by heating, in a pressure bomb, a THF solution of **10** in presence of hydrazine monohydrate and Pd/C, producing the unstable and colourless dodeca-amina-bistetraaza-calix[4]arene **11** (not isolated) that is subsequently oxidized by air to form the bis azacalixphyrin **4** as a dark solid in 30% yield (Scheme 1, see the ESI† for solid IR and solid state ^{13}C NMR spectra). The sufficient solubility of the fused macrocycle **4** in polar solvents allowed its purification through flash column chromatography on alumina. The structure of **4** was confirmed by its high-resolution mass spectrum (HRMS) showing a signal at m/z 1269.8496 [(M+H^{+})] (See the ESI†). DFT calculations (*vide infra*) conducted on the unsubstituted analogue (octyl chains removed) of **4** shows that **4** might exist, in solution, as a mixture of two conformers (see below) of neighbouring energies, each presenting several tautomeric forms in equilibrium due to intramolecular proton transfers between the peripheral amine and imine groups. The simultaneous presence of these multiple species in equilibrium is likely the reason why the different ^{1}H NMR spectra of **4** show only very broad signals despite the different solvents (including acidic ones) and temperatures used (see the ESI†). To ensure the presence of a single tautomer, i.e., a diprotonated form **4.H$_2$**$^{2+}$, the UV-Vis-NIR absorption spectrum of **4** was recorded in acidic MeOH and compared with the one of a solution of the simple ACP **2** in the same medium (Fig. 3.).[‡] As anticipated by *ab initio* calculations, the fusion of two ACP produces a redshift of all the absorption bands which is particularly significant when considering the NIR bands of **2.H$_2$**$^{2+}$ (λ_{max} = 894 nm) and **4.H$_2$**$^{2+}$ (λ_{max} = 1029 nm). This shift from the NIR-I to the NIR-II domain is also accompanied by a significant hyperchromic effect (**2.H$_2$**$^{2+}$: ε^{894} = 14 500 M^{-1}cm^{-1}, **4.H$_2$**$^{2+}$: ε^{1029} = 17 800 M^{-1}cm^{-1}).

We have further performed theoretical calculations to help rationalizing the obtained results, computational details can be found in the ESI†. As for the previously-studied monomeric **1-3**,[13,15,16,17] we could find several almost iso-energetic tautomers for the neutral form of **4** represented in Fig. 1 depending on the relative positions of the imine and amine groups. We will focus on the diprotonated form, **4.H$_2$**$^{2+}$, that show only one possible tautomer here (see the ESI† for other structures). We could find two conformers for **4.H$_2$**$^{2+}$: a S-shaped one, similar to the one of the precursor **10**, and a U-shaped structure (Fig. 4), the latter being only slightly less stable than the former (ΔG=1.7 kcal/mol). Obviously, the structures conserve the saddle-shape of the individual macrocycles[13] and are much flatten compared to **10**, illustrating their π-conjugated nature. The central CC bond, connecting the two macrocycles are ca. 1.48 Å long, that is, have mostly a single-bond character in the ground electronic state.
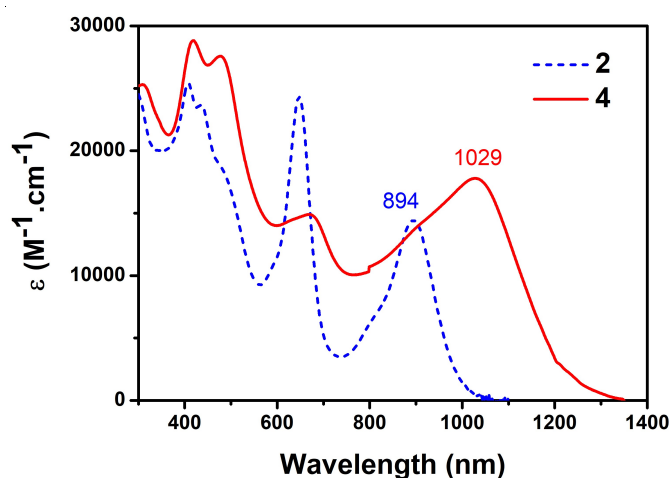

Fig. 3. UV-Vis-NIR electronic absorption spectra of ACP **2.H$_2$**$^{2+}$ (---) and of the bis-ACP **4.H$_2$**$^{2+}$ (—) in acidic MeOH.[‡]
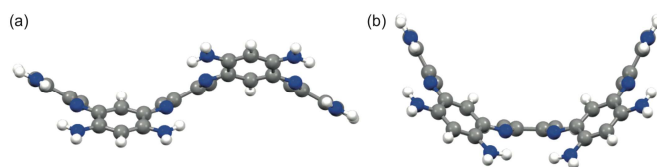
Fig. 4. Representation DFT geometries for the S- (a) and U-shaped (b) **4.H$_2$$^{2+}$** (octyl chains replaced by hydrogen atoms in the calculations)

The aromatic character of the individual macrocycles, as measured by the NICS(O) metric are -7.0 ppm and -6.3 ppm for the S- and U-shaped **4.H$_2$$^{2+}$** structures, respectively. These values are slightly smaller than in **1.H$_2$$^{2+}$** (-8.4 ppm). In the same time, all six-member cycles of **4** are anti-aromatic as in **1-3**, confirming that the Lewis structure displayed in Fig. 1 is qualitatively correct.

We have determined with Time-Dependent Density Functional Theory (TD-DFT) the transition energies for the first dipole-allowed excited-states. For **1.H$_2$$^{2+}$**, theory predicts a transition at 791 nm (*f*=0.24), which is blueshifted compared to experiment (894 nm, see Fig. 3), due to the lack of vibronic corrections in the calculations. This blueshift is -0.18 eV, typical of TD-DFT calculations. When going to **4.H$_2$$^{2+}$**, TD-DFT predicts absorptions at 866 nm (*f*=0.50) and 966 nm (*f*=0.41) for the S- and U-shaped conformers respectively. This corresponds to redshifts of -0.14 eV (S) or -0.28 eV (U) compared to the monomer, to be compared to the -0.18 eV measurement. Qualitatively, this can be explained by the topologies of the frontier orbitals displayed in Fig. 5. It is very clear that the frontier orbitals of the bis-ACP are totally delocalized over the whole structure and that the HOMO (LUMO) energy increases (decreases) significantly in going from the ACP to bis-ACP.
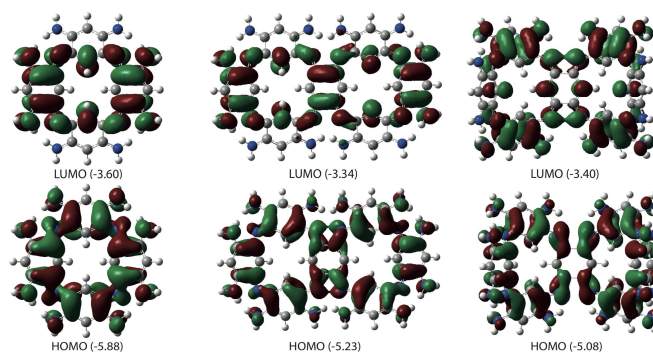

Fig. 5. Molecular orbitals (PBE0, isovalue = 0.02 a.u.) involved in the first dipole-allowed electronic transitions of (from left to right): **1.H$_2$$^{2+}$**, S-shaped **4.H$_2$$^{2+}$**, and U-shaped **4.H$_2$$^{2+}$**. The energies of the orbitals are given in eV.

In conclusion, we successfully synthesized the third example of a bis-azacalixarene where the two macrocycles share an aromatic bridging group.[19b] This compound is the crucial precursor of the first fused bis-azacalixphyrin. The communication between the two azacalixphyrin moieties produces a significant redshift of the absorption bands leading to an intense absorption band in the NIR-II domain comparable in positions and intensities to those observed in analogous fused bis-porphyrins. Future investigations will focus on the use of this new class of NIR-II dyes as PAI contrast agents.

Notes and references

‡ The nature of the solvent has a strong influence on the absorption profiles which is mainly due to the mixture of different protonated species in solution. Thus, 0.1 M trifluoroacetic acid (TFA) was added to the solutions to ensure the exclusive presence of diprotonated species (The spectra recorded in neutral and in basic MeOH are given in Figure S2 in the ESI†).

1 G. Qian and Z. Y. Wang, *Chem. Asian J.*, 2010, **5**, 1006.
2 (a) D. Li, Y. Hu, N. Zhang, Y. Lv, J. Lin, X. Guo, Y. Fan, J. Luo and X. Liu, *ACS Appl. Mater. Interfaces*, 2017, **9**, 36103; (b) H. Tachibana, N. Aizawa, Y. Hidaka and T. Yasuda, *ACS Photonics*, 2017, **4**, 223.
3 X. Zhang, T. Peng and S. Song, *J. Mater. Chem. A*, 2016, **4**, 2365.
4 P. Brogdon, H. Cheema and J. H. Delcamp, *ChemSusChem*, 2018, **11**, 86.
5 F. Verstraeten, S. Gielen, P. Verstappen, J. Kesters, E. Georgitzikis, J. Raymakers, D. Cheyns, P. Malinowski, M. Daenen, L. Lutsen, K. Vandewal and W. Maes, *J. Mater. Chem. C*, 2018, **6**, 11645.
6 (a) H. Lim, S. Seo, S. Pascal, Q. Bellier, S. Rigaut, C. Park, H. Shin, O. Maury, C. Andraud and E. Kim, *Sci. Rep.* 2016, **6**, 18867; (b) D.-H. Kim, A. D'Aléo, X.-K. Chen, A. D. S. Sandanayaka, D. Yao, L. Zhao, T. Komino, E. Zaborova, G. Canard, Y. Tsuchiya, E. Choi, J. W. Wu, F. Fages, J.-L. Brédas, J.-C. Ribierre and C. Adachi, *Nat. Photonics*, 2018, **12**, 98.

7   S. Pascal, Q. Bellier, S. David, P.-A. Bouit, S.-H. Chi, N. S. Makarov, B. Le Guennic, S. Chibani, G. Berginc, P. Feneyrou, D. Jacquemin, J. W. Perry, O. Maury and C. Andraud, *J. Phys. Chem. C*, **123**, 23661.

8   (a) G. Hong, A. L. Antaris and H. Dai, *Nat. Biomed. Eng.*, **1**, 0010; (b) F. Ding, Y. Zhan, X. Lu and Y. Sun, *Chem. Sci.*, 2018, **9**, 4370.

9   H. Zhu, P. Cheng, P. Chen and K. Pu, *Biomater. Sci.*, 2018, **6**, 746.

10 (a) Q. Miao and K. Pu, *Adv. Mater.*, 2018, **30**, 1801778; (b) Kenry, Y. Duan and B. Liu, *Adv. Mater.*, 2018, **30**, 1802394.

11 J. Fabian, H. Nakazumi and M. Matsuoka, *Chem. Rev.*, 1992, **92**, 1197.

12 (a) A. Muranaka, S. Ohira, D. Hashizume, H. Koshino, F. Kyotani, M. Hirayama and M. Uchiyama, *J. Am. Chem. Soc.*, 2012, **134**, 190; (b) N. Toriumi, N. Asano, T. Ikeno, A. Muranaka, K. Hanaoka, Y. Urano and M. Uchiyama, *Angew. Chem. Int. Ed.*, 2019, **58**, 7788; (c) X. Xue, A. Lindstrom and Y. Li, *Bioconjugate Chem.*, 2019, **30**, 1585.

13 Z. Chen, M. Giorgi, D. Jacquemin, M. Elhabiri and O. Siri, *Angew. Chem. Int. Ed.*, 2013, **52**, 6250.

14 T. D. Lash, *Org. Biomol. Chem.*, 2015, **13**, 7846.

15 (a) G. Marchand, A. D. Laurent, Z. Chen, O. SIri and D. Jacquemin, *J. Phys. Chem. A*, 2014, **118**, 8883; () G. Marchand, P. Giraudeau, Z. Chen, M. Elhabiri, O. Siri and D. Jacquemin , *Phys. Chem. Chem. Phys.*, 2016, **18**, 9608; (c) G. Marchand, O. Siri and D. Jacquemin, *Phys. Chem. Chem. Phys.*, 2016, **18**, 27308; (d) G. Marchand, O. Siri and D. Jacquemin, *Phys. Chem. Chem. Phys.*, 2017, **19**, 15903; (e) C. Azarias, S. Pascal, O. Siri and D. Jacquemin, *Phys. Chem. Chem. Phys.*, 2018, **20**, 20056.

16 Z. Chen, R. Haddoub, J. Mahé, G. Marchand, D. Jacquemin, J. Andeme Edzang, G. Canard, D. Ferry, O. Grauby, A. Ranguis and O. Siri, *Chem. Eur. J.*, 2016, **22**, 17820.

17 L. Lavaud, S. Pascal, K. Metwally, D. Gasteau, A. Da Silva, Z. Chen, M. Elhabiri, G. Canard, D. Jacquemin and O. Siri, *Chem. Commun.*, 2018, **54**, 12365.

18 (a) T. Tanaka and A. Osuka, *Chem. Soc. Rev.*, 2015, **44**, 943; (b) A. Tsuda, H. Furuta and A. Osuka, *J. Am. Chem. Soc.*, 2001, **123**, 10304.

19 (a) J. L. Katz, K. J. Selby and R. R. Conry, *Org. Lett.*, 2005, **7**, 3505; (b) G R. Haddoub, M. Touil, Z. Chen, J.-M. Raimundo, P. Marsal, M. Elhabiri and O. Siri, *Eur. J. Org. Chem.*, 2014, 745.

(a) H. Konishi, S. Hashimoto, T. Sakakibara, S. Matsubara, Y. Yasukawa, O. Morikawa and K. Kobayashi, *Tetrahedron Lett.*, 2009, **50**, 620; (b) G. Canard, J. A. Edzang, Z. Chen, M. Chessé, M. Elhabiri, M. Giorgi and O. Siri, *Chem. Eur. J.*, 2016, **22**, 5756.